

Complimentary split ring resonator sensor with high sensitivity based on material characterization

Amer Abbood Al-behadili¹, Teodor Petrescu², Iulia Andreea Mocanu³

^{1,2,3}Electronic Engineering, Telecommunications and Information Technologies Faculty,
University Politehnica of Bucharest, Romania

¹Electrical Engineering, College of Engineering, Mustansiriyah University Baghdad, Iraq

Article Info

Article history:

Received May 30, 2019

Revised Jul 2, 2019

Accepted Jul 18, 2019

Keywords:

Complementary split ring resonators (CSRRs)

Material characterization

Metamaterials

Non-invasive measurement

Planer sensor

ABSTRACT

A new model of microwave planar sensor established on the complementary split ring resonator (CSRR) as well as an air hole in substrate of the structure is introduced for a precise measurement of materials permittivity. The hole is filled into substrate of the planar microstrip line. The CSRR structure with hole is selected for the sensitivity analysis, the result is established to hold over quite sensitive compared with CSRR structure without hole and thus evidence to be more suitable for the sensor design. The sensor in the form of CSRRs operating at a 1.74–3.4 GHz band is explained. At resonance, it is found that the electric field produced straight the plane of CSRR being highly sensitive for the characterization of sample resident with the sensor. The minimum transmission frequency of sensor shifts from 3.4 to 1.74 GHz as the sample permittivity varies from 1 to 10. A numerical paradigm is introduced herein for the computation of the system resolution as a assignment of resonance frequency and sample permittivity using electromagnetic simulator. It is found that the proposed sensor provides 35% increment in sensitivity more than conventional sensor for same permittivity of the specimen.

This is an open access article under the [CC BY-SA](https://creativecommons.org/licenses/by-sa/4.0/) license.



Corresponding Author:

Amer Abbood Al-behadili,

Electronic Engineering, Telecommunications and Information Technologies Faculty,

University Politehnica of Bucharest,

București 060042, Romania.

Email: amer_osman@uomustansiriyah.edu.iq

1. INTRODUCTION

Permittivity is a fundamental material characteristic for large application such as quality control in the food industry, bio-sensing, properties of substrate and so on. Accurate computation of the permittivity is the most important task for microwave engineering in general. This is because the material response to electrical signals relies on the permittivity of materials. Several techniques have been proposed and employed for the permittivity characterization of material under test (MUT). These techniques can be categorized as free-space methods, near-field sensors, transmission-line methods and resonant cavity [1].

The free space method commonly employs the extremely directive lens and horn antennas laid on both sides of the MUT. The vector network analyzer (VNA) is connected to the antennas to measure the scattering parameters and phase constant to describe the specimen [2–5]. This technique has the advantage of being contactless and not wasteful, but it needs to employ of costly antennas and lenses, as well as the requirement of a big specimen.

Another technique for measurement of materials' permittivity is the transmission-line technique. In this technique, the MUT is used as a loading material for transmission lines. Such as, a slice of material can be incorporated to a waveguide [6, 7], or the depositing coaxial line materials can be substituted by the MUT [8]. The scattering parameters from the MUT-filled region provide the data necessities for extraction of material properties. This technique is comparatively low expense than the free-space technique. However, the sensitivity of the scattering parameters process is not quite efficient for low loss specimens and the specimen elaboration is also highly oftentimes a challenging mission [9]. The structures of stripline and microstrip-line are also used for this technique [10–12]. The quite accurate technique is the resonant cavity method [13, 14]. In this method, a cavity resonator is loaded with the MUT, and the shift in the resonance frequency and the variation in the quality factor are computed. Circular resonators and microstrip-line resonators also have been employed for this purpose [15, 16], other than a traditional box resonator. This technique also needs accurate sample elaboration.

In the last few years, the resonant planer sensors based on complementary split ring resonator (CSRR) coupled to planer microstrip line have been investigated to determine the permittivity of the MUT [17–23]. The layout of the resonant planer sensor has obviously numerous features such as portability, the low expense, being non-invasive and ease in specimen elaboration. However, all these structures of resonant planer sensor are based on one specified solid substrate, in which the value of the effective permittivity of this substrate has an important role in computing resonance frequency of the structure. Through the investigation of previous characterization techniques, determination accuracy of the real permittivity of MUT depends on frequency shift value of the sensor resonant frequency due to loading sample, and this frequency shift value which is provided by planar sensors based on CSRR is confined and restricted according to the design criteria of the planer sensors such as the relative permittivity of sensors substrate in addition to the physical dimensions of CSRR. Therefore, the precision of calculation is limited by this value. For this reason, a microstrip planer sensor with specified substrate filled by air hole is proposed here. Hence a structure with low effective permittivity of substrate is achieved, where it is founded later after careful verification that this technique improves the precise of materials characterization employing the planer sensors based CSRR.

The geometry of air hole is selected only after proceeding the elaborated sensitivity test where it is detected that the CSRR unit cell have substrate with air hole provides preferable sensibility in comparison with the CSRR unit cell without hole possessing the identical unit area. This return is also proved with the aid of electromagnetic analytical terms. The suggested technique is established on the layout and development of a microstrip established circular CSRR resonant sensor, which depicts the characteristics approach to a stop band filter. For workout method, the MUT is put on the ground plane of the microstrip line in which it covers the total CSRR area. The proposed planer sensor is modeled and simulated employing the numerical electromagnetic solver, the High Frequency Structure Simulator (HFSS). The precision of the developed technique is investigated using the data obtained from conventional structure possessing identical unit area. The suggested sensor is simulated on a FR4 substrate and is point to be active in the range of frequency 1.74 to 3.4 GHz.

2. THEORY

For traditional microwave resonator established method, the overall expressions narrative the variation in resonant frequency for permeability and permittivity of the specimen under test are given as shown in (1) [24]:

$$\frac{\Delta f_r}{f_r} = \frac{\int_{vc} (\Delta \epsilon E_1 \cdot E_0 + \Delta \mu H_1 \cdot H_0) dv}{\int_{vc} (\epsilon_0 |E_0|^2 + \mu_0 |H_0|^2) dv} \quad (1)$$

where, vc is the cavity volumes, Δf_r represent the change in resonant frequency, $\Delta \epsilon$ and $\Delta \mu$ are the change in complex permittivity and complex permeability, respectively, add to that ϵ_0 is the free space permittivity, while μ_0 perform permeability of the free space. The characters E_0 , H_0 represent the electric and the magnetic fields of the hollow cavity meanwhile E_1 , H_1 perform the electric and the magnetic fields, respectively down loaded situation. In the case of dielectric materials, the variation in complex permeability ($\Delta \mu$) approach to be zero. A well as, the stored energy, E and H fields in the resonant structure should be similar at the resonant frequency. Under the two previous situations, term (1) is modified as shown in (2):

$$\frac{\Delta f_r}{f_r} = \frac{\int_{vc} \Delta \epsilon E_1 \cdot E_0 dv}{2 \int_{vc} \epsilon_0 |E_0|^2 dv} \quad (2)$$

where, v_c is the volume of the sample. The previous expressions (1) and (2) are essentially being employed in situation of the waveguide cavities, in which the electromagnetic field expressions with and without material disorder, can be readily derived. But it is complicated to use this notion for the CSRR structures which are electrically small resonators. A lot of study groups possess suggested various geometries of CSRR in the last few years [10, 19]. However, in material description, the sensibility of the microstrip sensor is of main interest, which is then related with the magnetic and the electric field intensity exist across the planar geometry. For this purpose, in this work, two CSRR unit cells, with and without hole are compared for the sensibility test employing the HFSS.

3. DESIGN AND ANALYSIS OF THE STRUCTURE

The proposed structure is one type of the quasi-static consist of substrate with hole and split rings in two ports in which an inductance stimulated by circulating current in the rings and the effective capacitance increased across the space through the rings, hence electrically small resonator is achieved. To detail the performance of the proposed structure, a comparison must be made with traditional structure and verify the results of each structure. The configuration of two substrates of CSRR unit cells without and with hole are depicted in Figures 1 (a) and (b), respectively.

The layout and design parameters of CSRR unit cell with hole in substrate are depicted in Figure 2 (a) and Figure 1 (b), respectively. The equivalent circuit of CSRR unit cell is represented in Figure 2 (c), where L and C are the microstrip line per-unit-cell inductance and capacitance, and electrical coupling on the ground represented by all total capacitance and inductance of CSRR which are C_c and L_c . Figure 2 (c), depicts the per-unit-cell capacitance, C is variable capacitance, because it will be extracted from the change in material substrate due to the hole existence. The resonant frequency of the equivalent circuit is given as shown in (3) [25, 26]:

$$f_r = \frac{1}{2\pi\sqrt{L_c(C+C_c)}} \quad (3)$$

where f_r represents minimum transmission frequency of the structure. To clarify all details, the proposed structure in Figure 2 (a) has been designed as follows: the thickness of FR4 substrate is 1.6 mm with a cross-sectional dimension 12×12 mm, is used to sample the suggested CSRR unit cell. The CSRR design parameters possessed in the simulation are $d, s = 0.76$ mm, $r_{ext} = 5.32$ mm (Figure 2 (b)). At each ring, the width of the slit (g) is 0.61 mm and thickness of microstrip line and ground plane (t) is 0.035 mm.

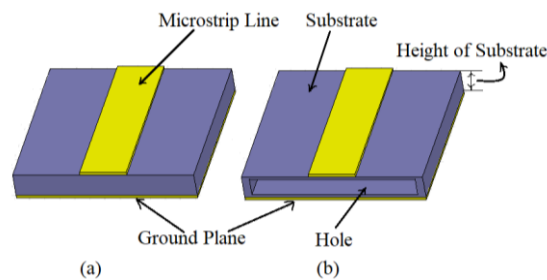


Figure 1. Layout structure of substrate of CSRR unit cell: (a) without hole (traditional layout), (b) with hole

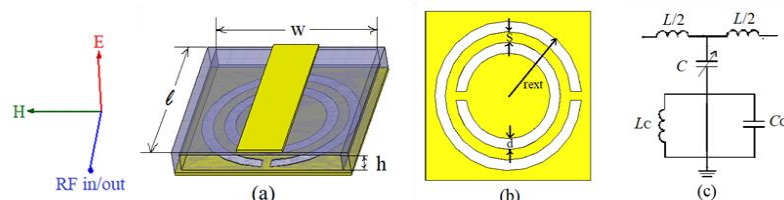


Figure 2. (a) Layout structure of CSRR unit cell with hole in substrate, (b) Topology of CSRR, (c) Equivalent circuit of the structure

The shape and dimensions of the hole are carried out according to the maximum possible shifting can be achieved in minimum transmission frequency (S_{21} resonance frequency) compared with that obtained in

traditional structure (taking into consideration of the change in insertion loss (ΔS_{21}) and the ability of design). Since the hole is etching gap in substrate of CSRR unit cell so the changes in values of hole dimensions ($\ell \times w \times h$) will affect the properties of the substrate structure, thus all parameters which are the function of substrate will change. Behavior of change in parameters due to changes in values of hole dimensions are depicted Figures 3, 4, 5 and 6.

The calculation of both per-unit-cell L and C depends on both length and height of substrate per unit cell ($\ell \times h$) [27], so the change in hole volume will be represented by the change in hole area ($\ell \times h$) multiply by proposed width dimension (w) (see Figure 2 (a)) as a constant value (in which cover external radius of CSRR). The results in Figure 3 depict the increase in the area of air hole leading to reduction of the per-unit-cell capacitance which was filled of FR4 medium. In the same time the per-unit-cell capacitance of air medium is increased. This happens due to the raising of the air hole volume (ℓ is varying from 0 to 12mm, h is varying from 0 to 1.2mm while w is fixed at 11mm), and hence the per-unit-cell capacitance of air hole will be the dominant medium ($C_t = C_1 + C_2 \approx C_2$ with $\epsilon_r = 1$).

Figure 4 demonstrates that at the maximum dimensions of the hole volume ($(\ell \times h = 14.4) \times w$), the value of the per-unit-cell inductance related with air hole is less than the inductance value when using FR4 substrate (without hole). The reason is due to inductance expression which is a proportional function of the substrate height (h), as is known FR4 substrate height (1.6 mm) is greater than the maximum height dimension of hole (1.2 mm).

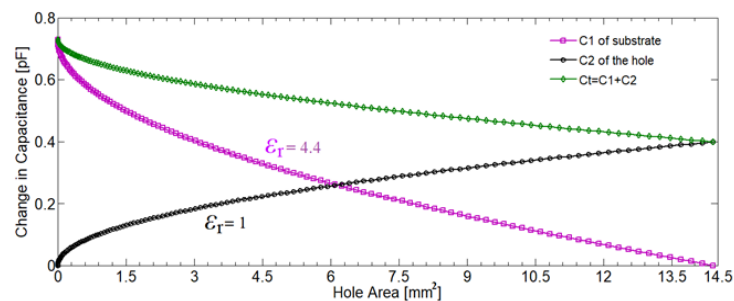


Figure 3. Changes of both per-unit-cell capacitances, C_s for FR4 and air hole etched due to varying in the hole area

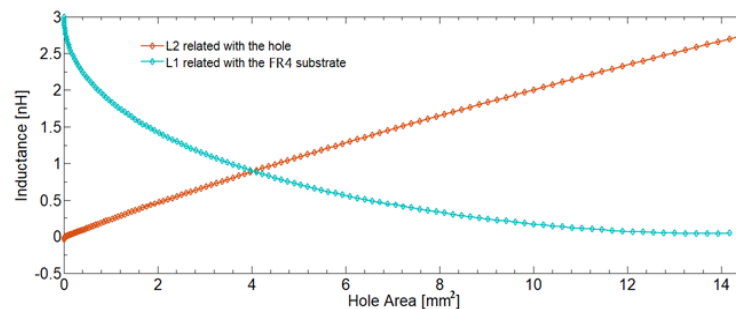


Figure 4. Changes of both per-unit-cell inductance, L_s for FR4 and air hole etched due to varying in the hole area

The most important change that must be prominent is the change of resonant frequency of the structure (compared with resonant frequency of the structure without hole), which is explained in Figure 5. It can be seen that the resonant frequency shifts to higher frequencies when the volume hole increases (dominant air hole medium at maximum increment), also it can be note the maximum difference in insertion loss is less than 0.5 dB compared with reference resonance frequency (at the structure without hole).

The main purpose of this investigation is to obtain a highly sensitive unit cell for permittivity characterization. Therefore, the select of the hole dimensions will be based on which are most affected by changes in the surrounding medium of the structure. To achieve this verification, the resonance frequency is assumed the reference frequency when the structure is surrounded by vacuum, whenever ϵ_r of the medium is changed, the frequency shifts with respect to the reference frequency. This procedure is repeated for each

change in dimensions of the hole. Note that, the change in the surrounding medium is achieved by changing the permittivity of the radiated box (vacuum permittivity will be the reference permittivity) of the structure.

From the results presented in Figure 6, the hole with maximum dimensions is more sensitive to variation in permittivity than the hole with less dimensions, as well as at maximum hole dimensions the performance of insertion loss was not being affected much as shown in Figure 5. Therefore, the hole dimensions are selected as: $\ell = 12$ mm, $w = 11$ mm and $h = 1.2$ mm for the unit cell have cross-sectional dimension 12×12 mm, to be analyzed moreover for the aim of permittivity description.

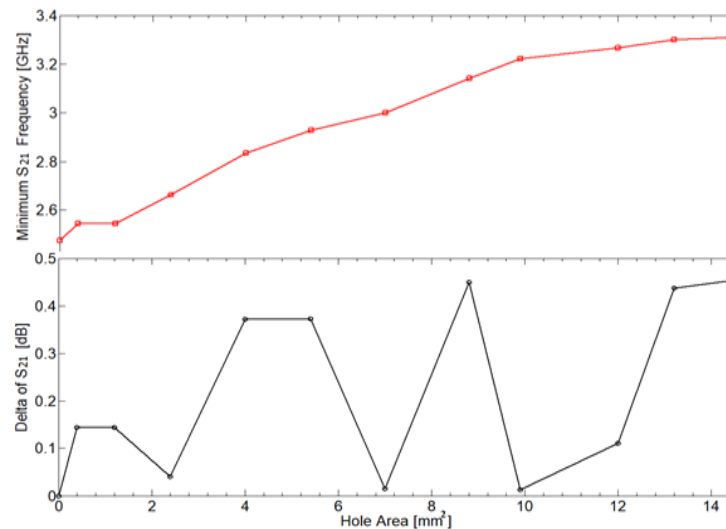


Figure 5. Permittivity phase response and magnitude of transmission zero frequency (S_{21}) of CSRR unit cell

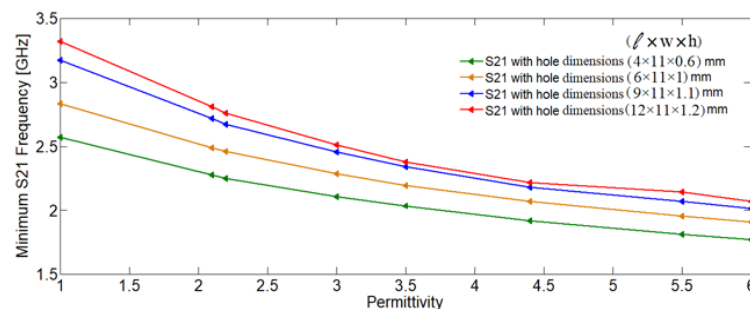


Figure 6. Resonance of S_{21} frequency with varying of permittivity at different dimensions of the hole

4. COMPARISON AND ANALYSIS SENSITIVITY OF CSRR UNIT CELL WITH AND WITHOUT HOLE

For an adjuster comparison between the suggested structure and traditional CSRR unit cell, the unit cell areas in addition to the layout parameters in Figure 2 (b) are taken as identical throughout this discussion. Initially both structures are modeled and the simulation is completed to achieve the scattering parameter (S_{21}) in the band of specified frequency. The per-unit-cell inductance and capacitance (L , C) which related to the type of permittivity of the structure (at air hole) are obtained from Figures 3 and 4, while L_C and C_C of both structures are calculated by [26]. The computed lumped parameters are depicted in Table 1.

It is important to note from Table 1 that the value of L_C related with the proposed structure is much smaller than in traditional CSRR unit cell, at the same time it can be observed L_C is the most affected parameter due to presence of the hole as compared with other parameters. This essentially denotes that as expression (3), the resonant frequency of the proposed structure will be vastly higher than the traditional structure. This can also be explained by the actuality that the resonant frequency of such resonators in fact increase with decreasing value of permittivity of structure. After calculating equivalent circuit parameters, results of sensitivity analysis which represented by varying the medium surrounding both structures are carried out in Figure 7. From Figure 7 it can be concluded that the suggested structure is quite sensitive to

variation in permittivity compared with traditional structure. However, for further evaluation, the two structures will be used to establish two models as planer sensors to be analyzed moreover for the aim of permittivity description.

Table 1. Lumped parameters extracted for both structures

Lumped Parameters	Traditional CSRR unit Cell	Proposed Structure
L (nH)	3	2.76
C (pF)	0.67	0.4
C_c (pF)	1.28	2
L_c (nH)	2.255	0.97

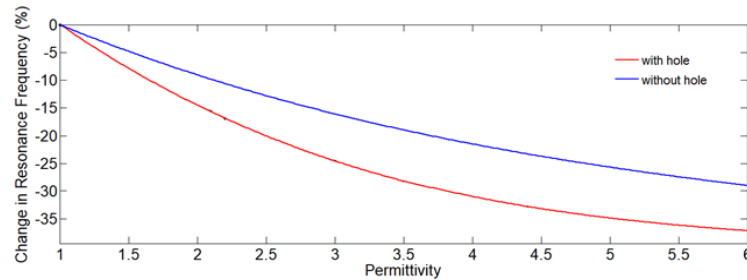


Figure 7. Behaviors of Proposed structure and CSRR unit cell for permittivity changes in the surrounding medium. The relative f_r shift is computed according to the reference f_r in case of the medium is vacuum

5. DESIGN CONSIDERATION

Before starting the model of the sensor it is necessary to refer to some of the basics that may have an effect on the performance of the sensor, hence the sensitivity will reduce. The direction of the open ends of the hole that etched into the substrate plays an important role in the design of the structure. As indicated in Figure 2 (a), the orientation of the open ends is parallel to the input and output ports (i.e., perpendicular to the excitation of magnetic field). Thus, in order to avoid affecting the performance of insertion loss, as shown in Figure 8 which depicts two behaviors of S_{21} of the structure, one for the hole positioned in parallel and the other in perpendicular with plane of magnetic field excitation. From the above illustration it can be concluded that the open ends of the hole should be parallel to the input and output ports (along the microstrip line) and this requires drilling the substrate along the entire transmission line between two ports and this is very difficult to achieved in addition to impact of sensor performance. In order to avoid this dilemma a new structure with bending microstrip line will be proposed and all details of design and sensitivity analysis are depicted in the next few sections.

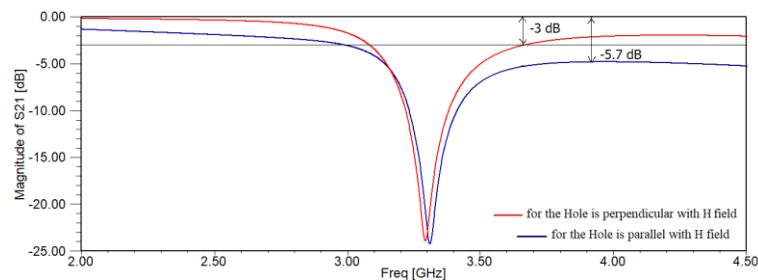


Figure 8. Behavior of S_{21} for the structure in Figure 2 with respect of two orientation status of the hole

6. DECIDING OF THE SENSOR MODEL

Due to the change in the permittivity of the material under test (MUT), the capacitance of CSRR will change hence a shifting in resonance frequency is obtained (the inductance of the CSRR is counted to be constant in condition of dielectric materials). In current paper, two proposed structures (one with hole as shown in Figure 9 and the other without hole) possessing similar unit cell area, are investigated for the sensitivity test, and detailed verification is presented in following sections. The proposed sensor in Figure 9 has (24×30 mm) external cross section area, with folded microstrip line in order to make the hole in

the substrate as low as possible while keeping the orientation of open ends perpendicular to the excitation of magnetic field. All remaining design parameters will be the same that in Figure 2.

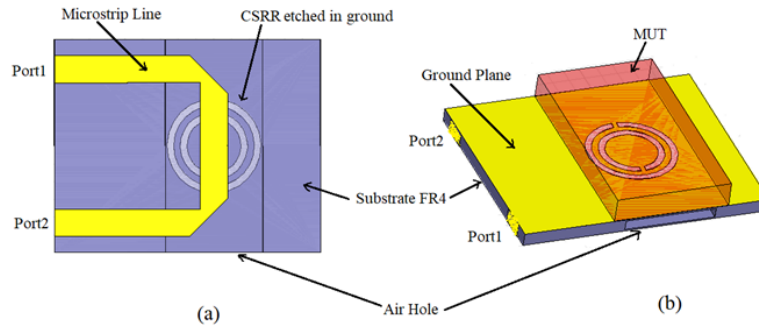


Figure 9. Layout of proposed planer sensor: (a) top view with diaphanous substrate, (b) sight view of the structure with MUT putted atop ground plane

7. SENSOR ANALYSIS

In order to highlight the performance of the proposed sensor in Figure 9, an identical sensor without hole has been modeled and both sensors are analyzed and investigated. The transmission coefficient is computed using full wave simulation (HFSS) for reference case (sensors without load of MUT). The magnitudes of the S_{21} -parameter are depicted in Figure 10. Minimum transmission coefficient of sensor without hole at 2.35 GHz (f_r), while it experiences a minimum value at 3.42 GHz (f_h) for sensor with hole. In addition, it can be observed the design effect on the performance of S_{21} behavior as illustrated in section 3. The computed minimum transmission frequencies in Figure 10 will be used as the reference frequencies to determine the shifting in frequency due to interference of the permittivity of MUT. Figure 11 depicts that f_h (resonance frequency of proposed sensor) shifts 47.2% and f_r (resonance frequency of traditional sensor) shifts 33.96% when the permittivity of the specimen varies from 1 to 10.

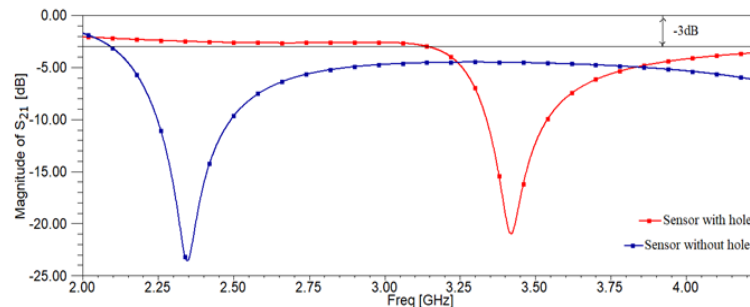


Figure 10. Transmission coefficient magnitude as a function of frequency. This response is obtained for unloaded MUT

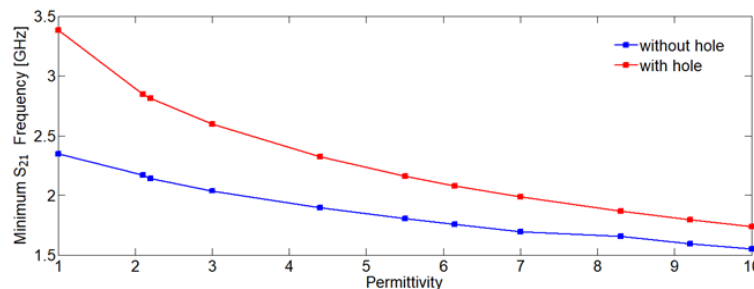


Figure 11. Values of f_h and f_r with respect to permittivity change. As varying permittivity from 1 to 10, f_h record large shift compared with f_r

Further sensitivity analysis is represented by quantifying the resolution (as the same procedure followed in [21]) of both sensors to validate the proposed sensor for determining permittivity. From Figure 11 the shift in resonance frequencies f_h and f_r is a data which is associated with permittivity of the MUT (ϵ_{MUT}). The resolution relies on derivative of ϵ_{MUT} with respect to f_h and f_r . The expression for the reliance of ϵ_{MUT} on f_h and f_r can be achieved by using curve fitting tool for the data presented in Figure 11. The polynomials obtained are given by (4) and (5) as follows:

$$\epsilon_{MUT} = -1.717(f_h)^3 + 16.67(f_h)^2 - 55.88(f_h) + 65.74 \quad (4)$$

$$\epsilon_{MUT} = -9.09(f_r)^3 + 64.11(f_r)^2 - 156.2(f_r) + 132.1 \quad (5)$$

and the derivative of ϵ_{MUT} with respect to f_h and f_r are computed as:

$$\frac{\partial \epsilon_{MUT}}{\partial f_h} = -5.15(f_h)^2 + 33.34(f_h) - 55.88 \quad (6)$$

$$\frac{\partial \epsilon_{MUT}}{\partial f_r} = -27.27(f_r)^2 + 128.22(f_r) - 156.2 \quad (7)$$

A value for the effective range of the sensor utilized for measurement should be assumed. This hypothesis demonstrates the accuracy of the sensor that is used for measuring the transmission coefficients. Suppose that the precision of the system or sensor that is being utilized to gauge f_h and f_r is 40-MHz. By using this hypothesis and (6) and (7), the variation in the permittivity $\Delta\epsilon$ that corresponds to a 40-MHz shift in f_h and f_r are computed. 40-MHz is a moderate choice for accuracy. Figure 12 depicts the resolution of the two sensors as a function of MUT permittivity. As the permittivity of MUT increases, the resolution is reduced. When $\epsilon_{MUT} = 1$, a 40-MHz shift in f_h compensates to $\Delta\epsilon = 0.005$. At $\epsilon_{MUT} = 10$, a 40-MHz shift in f_h compensates to $\Delta\epsilon = 0.0325$.

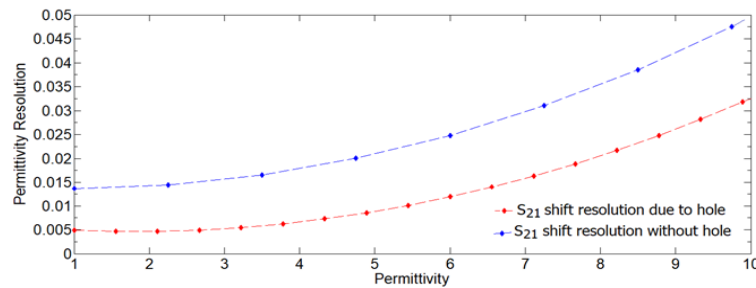


Figure 12. Permittivity decision as a function of MUT permittivity. It can be computed by determining the desired permittivity change to result a 40-MHz shift in f_h and. The resolution is reduced when MUT permittivity is increased

8. DEPOSITION OF SAMPLE PERMITTIVITY

It is obvious to know the effect of MUT loading sensor is observed in idiom of the resonant frequency of the suggest sensor as discussed previously. Refer to the (1), the inverse square of resonant frequencies, taken away from the simulated data of S_{21} of (3), the inverse square of resonant frequencies, taken away from the simulated transmission coefficient data (Figure 11), are plotted with the corresponding specimen permittivity as depicted in Figure 13. It can be seen the fluctuation of $(f_h)^{-2}$ and $(f_r)^{-2}$ with ϵ_{MUT} is linear. As indicated in section 4, the region of the sensor which loaded by MUT has capacitance proportional to the permittivity of MUT and hence, the inverse square of the resonant frequency is directly proportional to the MUT permittivity (as spotted in (3)), i.e. $\epsilon_{MUT} \propto (f_h)^{-2}$ and $(f_r)^{-2}$. Therefore, in order to integrate all the above substance, the permittivity of MUT mathematically represented as follow:

$$\epsilon_{MUT} = -118.9(f_h^{-2})^3 + 87.14(f_h^{-2})^2 + 17.9f_h^{-2} - 1.176 \quad (8)$$

expression (8) is obtained utilizing the tool of curve fitting, which prepares a numerical paradigm of the suggested sensor to determine the real permittivity of specimen in terms of the recorded resonant frequency.

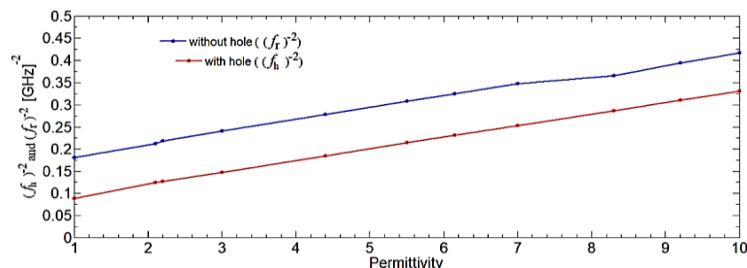


Figure 13. Relationship between MUT permittivity and transmission coefficient of proposed and traditional sensors is used for the standardization of the sensor

9. COMPARISON RESULTS OF CSRR PLANER SENSORS WITH AND WITHOUT HOLE

After standardization, a number of materials are described using the suggested sensors. Resonant frequencies of S_{21} data for all conditions are recorded using HFSS. The simulated results are also compared with the criterion data obtainable in the reference [21] which are given in columns 2 of Table 2.

From Table 2 it can be deduced that the proposed sensor with hole in substrate presents frequency shift values greater than in conventional sensors. Hence the proposed sensor provides 35% increment in sensitivity more than conventional planer sensors have the same relative permittivity of the substrate (without hole). And about 26% increment in sensitivity more than conventional planer sensors have low loss Rogers substrate (without hole) [21].

Table 2. Simulated results of variation resonant frequencies using proposed CSRR and conventional CSRR based planer sensor techniques

Technique Materials ↓	Reference values of the sample [21]	Δf_r (Air-MUT) [GHz]	Proposed sensor based CSRR without hole. [GHz]	Δf_r (Air-MUT) [GHz]	Proposed sensor based CSRR with hole. [GHz]	Δf_r (Air-MUT) [GHz]
Air($\epsilon_r = 1$, $\tan\delta = 0$)	$f_r = 1.15$ GHz	0	$f_r = 2.35$ GHz	0	$f_r = 3.42$ GHz	0
Teflon($\epsilon_r = 2.1$, $\tan\delta = 0.001$)	$f_r = 1.095$ GHz	0.055	$f_r = 2.173$ GHz	0.177	$f_r = 2.844$ GHz	0.576
RO3003($\epsilon_r = 3$, $\tan\delta = 0.0013$)	$f_r = 1.05$ GHz	0.1	$f_r = 1.897$ GHz	0.453	$f_r = 2.612$ GHz	0.808
FR4($\epsilon_r = 4.4$, $\tan\delta = 0.02$)	$f_r = 0.95$ GHz	0.2	$f_r = 1.695$ GHz	0.655	$f_r = 2.33$ GHz	1.09
Max. frequency shift when ϵ_r change from 1 to 10	37.5%	---	34%	---	47.2%	---
Structure cross section (cm x cm)	10x5	---	2.4x3	---	2.4x3	---

10. CONCLUSION

A new model of microwave planar sensor established on the complementary split ring resonator (CSRR) as well as an air hole in substrate of the structure is introduced for a precise measurement of materials permittivity. The CSRR is etched in the ground plane, while the hole is filled into substrate of the planar microstrip line. Two CSRRs structures with and without hole are selected for the sensitivity analysis, where the final is establish to hold over quite sensitivity and thus evidence to be more suitable for the sensor layout. The minimum transmission frequencies for each structure are observed relied on the permittivity of the specimen. A sensor in the form of CSRRs operating at a 1.74–3.4 GHz band is explained. At resonance, it is found that the electric field produced straight the plane of CSRR being highly sensitive for the characterization of sample resident with the sensor. The minimum transmission frequency of sensor shifts from 3.4 to 1.74 GHz as the sample permittivity varies from 1 to 10. A numerical model is introduced here for the computation of the system resolution as a function of resonance frequency and sample permittivity using electromagnetic simulator. It is found that the proposed sensor provides 35% increment in sensitivity more than conventional sensor for the same permittivity of the specimen.

REFERENCES

- [1] Rammah A., Zakaria Z., Ruslan E., Isa A. A., "Comparative study of materials characterization using microwave resonators," *Australian Journal of Basic and Applied Sciences*, vol. 9, no. 1, pp. 76-85, 2015.
- [2] D. K. Ghodgaonkar, V. V. Varadan and V. K. Varadan, "Free-space measurement of complex permittivity and complex permeability of magnetic materials at microwave frequencies," *IEEE Transactions on Instrumentation and Measurement*, vol. 39, no. 2, pp. 387-394, Apr 1990.

- [3] P. K. Kadaba, "Simultaneous Measurement of Complex Permittivity and Permeability in the Millimeter Region by a Frequency-Domain Technique," *IEEE Transactions on Instrumentation and Measurement*, vol. 33, no. 4, pp. 336-340, Dec 1984.
- [4] A. Khosrowbeygi, H. D. Griffiths and A. L. Cullen, "A new free-wave dielectric and magnetic properties measurement system at millimetre wavelengths," *1994 IEEE MTT-S International Microwave Symposium Digest (Cat. No.94CH3389-4)*, San Diego, CA, USA, vol. 3, pp. 1461-1464, 1994.
- [5] M. A. B. Aris and D. K. Ghodgaonkar, "Nondestructive and noncontact dielectric measurement method for high-loss liquids using free space microwave measurement system in 8-12.5 GHz frequency range," *2004 RF and Microwave Conference (IEEE Cat. No.04EX924)*, Selangor, Malaysia, pp. 169-176, 2004.
- [6] Erentok A., Ziolkowski R. W., Nielsen J. A., Gregor R. B., Parazzoli C. G., Tanielian M. H., Cummer S. A., Popa B. I., Hand T., Vier D. C., Schultz S., "Low frequency lumped element-based negative index metamaterial," *Applied Physics Letters*, vol. 91, no. 18, pp. 184104, 29 Oct 2007.
- [7] M. J. Akhtar, L. E. Feher and M. Thumm, "A waveguide-based two-step approach for measuring complex permittivity tensor of uniaxial composite materials," *IEEE Transactions on Microwave Theory and Techniques*, vol. 54, no. 5, pp. 2011-2022, May 2006.
- [8] C. A. Jones, J. H. Grosvenor and C. M. Weil, "RF material characterization using a large-diameter (76.8 mm) coaxial airline," *13th International Conference on Microwaves, Radar and Wireless Communications. MIKON - 2000. Conference Proceedings (IEEE Cat. No.00EX428)*, Wroclaw, Poland, vol. 2, pp. 417-420, 2000.
- [9] P. M. Narayanan, "Microstrip Transmission Line Method for Broadband Permittivity Measurement of Dielectric Substrates," *IEEE Transactions on Microwave Theory and Techniques*, vol. 62, no. 11, pp. 2784-2790, Nov 2014.
- [10] W. Barry, "A Broad-Band, Automated, Stripline Technique for the Simultaneous Measurement of Complex Permittivity and Permeability," *IEEE Transactions on Microwave Theory and Techniques*, vol. 34, no. 1, pp. 80-84, Jan 1986.
- [11] Heping Yue, K. L. Virga and J. L. Prince, "Dielectric constant and loss tangent measurement using a stripline fixture," *1998 Proceedings. 48th Electronic Components and Technology Conference (Cat. No.98CH36206)*, Seattle, WA, USA, pp. 1077-1082, 1998.
- [12] P. Queffelec, P. Gelin, J. Gieraltowski and J. Loaec, "A microstrip device for the broad band simultaneous measurement of complex permeability and permittivity," *IEEE Transactions on Magnetics*, vol. 30, no. 2, pp. 224-231, Mar 1994.
- [13] J. Baker-Jarvis *et al.*, "Dielectric characterization of low-loss materials a comparison of techniques," *IEEE Transactions on Dielectrics and Electrical Insulation*, vol. 5, no. 4, pp. 571-577, Aug 1998.
- [14] B. Milovanovic, S. Ivkovic and V. Tasic, "A simple method for permittivity measurement using microwave resonant cavity," *12th International Conference on Microwaves and Radar. MIKON-98. Conference Proceedings (IEEE Cat. No.98EX195)*, Krakow, Poland, vol. 3, pp. 705-709, 1998.
- [15] D. Shimin, "A New Method for Measuring Dielectric Constant Using the Resonant Frequency of a Patch Antenna," *in IEEE Transactions on Microwave Theory and Techniques*, vol. 34, no. 9, pp. 923-931, Sep 1986.
- [16] P. A. Bernard and J. M. Gautray, "Measurement of dielectric constant using a microstrip ring resonator," *IEEE Transactions on Microwave Theory and Techniques*, vol. 39, no. 3, pp. 592-595, Mar 1991.
- [17] Nelson SO, Trabelsi S. Influence of water content on RF and microwave dielectric behavior of foods. *Journal of Microwave Power and Electromagnetic Energy*, vol. 43, no. 2, pp. 13-23, 1 Jan 2008.
- [18] C. Lee and C. Yang, "Thickness and Permittivity Measurement in Multi-Layered Dielectric Structures Using Complementary Split-Ring Resonators," *IEEE Sensors Journal*, vol. 14, no. 3, pp. 695-700, Mar 2014.
- [19] Hardinata S, Deshours F, Alquíé G, Kokabi H, Koskas F, "Miniaturization of Microwave Biosensor for Non-invasive Measurements of Materials and Biological Tissues," *3rd International Seminar on Science and Technology (ISST) 2017*, pp. 90-93, 2017.
- [20] C. Lee and C. Yang, "Complementary Split-Ring Resonators for Measuring Dielectric Constants and Loss Tangents," *in IEEE Microwave and Wireless Components Letters*, vol. 24, no. 8, pp. 563-565, Aug 2014.
- [21] M. S. Boybay and O. M. Ramahi, "Material Characterization Using Complementary Split-Ring Resonators," *in IEEE Transactions on Instrumentation and Measurement*, vol. 61, no. 11, pp. 3039-3046, Nov 2012.
- [22] Albishi A, Ramahi O., "Detection of surface and subsurface cracks in metallic and non-metallic materials using a complementary split-ring resonator," *Sensors*, vol. 14, no. 10, pp. 19354-19370, 2014.
- [23] M. A. H. Ansari, A. K. Jha and M. J. Akhtar, "Design and Application of the CSRR-Based Planar Sensor for Noninvasive Measurement of Complex Permittivity," *IEEE Sensors Journal*, vol. 15, no. 12, pp. 7181-7189, Dec 2015.
- [24] Pozar D. M., "Microwave engineering," 3rd John Wiley & Sons, 2009.
- [25] Durán-Sindreu M., Naqui J., Bonache J., Martín F., "Split rings for metamaterial and microwave circuit design: A review of recent developments," *International Journal of RF and Microwave Computer-Aided Engineering*, vol. 22, no. 4, pp. 439-458, 2012.
- [26] J. Bonache, M. Gil, I. Gil, J. Garcia-Garcia and F. Martin, "On the electrical characteristics of complementary metamaterial resonators," *IEEE Microwave and Wireless Components Letters*, vol. 16, no. 10, pp. 543-545, Oct 2006.
- [27] Bahl I. J., "Lumped elements for RF and microwave circuits," Artech house, pp. 24-27, 2003.